

Developing a microspectrophotometer to measure the dependence of broadband refractive indices on Ge-doped concentrations in GRIN rods

Chun-Jen Weng,^{1,2} Ken-Yuh Hsu,¹ Cheng-Yeh Lee,³ and Yung-Fu Chen^{3,*}

¹*Department of Photonics & Institute of Electro-Optical Engineering, National Chiao Tung University, 1001 Ta-Hsueh Road, Hsinchu 30050, Taiwan*

²*Instrument Technology Research Center, National Applied Research Laboratories, Taiwan*

³*Department of Electrophysics, National Chiao Tung University, Taiwan*

yfchen@cc.nctu.edu.tw

Abstract: A confocal microspectrophotometer is utilized to scan the surface reflectivities of a polished gradient-index (GRIN) rod in the range of 400 to 900 nm. The pure fused silica is used to be a reference standard for deducing the absolute reflectivities of the Ge-doped core. Then, multi-wavelength refractive index profiles of the Ge-doped core can be further determined based on the Fresnel equation. Moreover, this work shows a connection between the material dispersion of the GRIN rod and the Ge-doped concentrations measured by an energy dispersive spectrometer. Finally, the dependence of the refractive index of the Ge-doped core on the doping concentrations at a certain wavelength can be easily expressed as a linear form.

©2015 Optical Society of America

OCIS codes: (300.6490) Spectroscopy, surface; (120.0120) Instrumentation, measurement, and metrology; (110.2760) Gradient-index lenses.

References and links

1. J. C. Jung and M. J. Schnitzer, "Multiphoton endoscopy," *Opt. Lett.* **28**(11), 902–904 (2003).
 2. T. Xie, S. Guo, Z. Chen, D. Mukai, and M. Brenner, "GRIN lens rod based probe for endoscopic spectral domain optical coherence tomography with fast dynamic focus tracking," *Opt. Express* **14**(8), 3238–3246 (2006).
 3. M. Zickar, W. Noell, C. Marxer, and N. de Rooij, "MEMS compatible micro-GRIN lenses for fiber to chip coupling of light," *Opt. Express* **14**(10), 4237–4249 (2006).
 4. Y. Kokubun and K. Iga, "Refractive-index profile measurement of preform rods by a transverse differential interferogram," *Appl. Opt.* **19**(6), 846–851 (1980).
 5. Y. L. Chen, H. C. Hsieh, W. T. Wu, W. Y. Chang, and D. C. Su, "Alternative method for measuring the full-field refractive index of a gradient-index lens with normal incidence heterodyne interferometry," *Appl. Opt.* **49**(36), 6888–6892 (2010).
 6. V. I. Vlad, N. I. Pallas, and F. Bociort, "New treatment of the focusing method and tomography of the refractive index distribution of inhomogeneous optical components," *Opt. Eng.* **35**(5), 1305–1310 (1996).
 7. E. Acosta, R. Flores, D. Vazques, S. Rios, L. Garner, and G. Smith, "Tomographic method for measurement of the refractive index profile of optical fibre preforms and rod GRIN lenses," *Jpn. J. Appl. Phys.* **41**(7), 4821–4824 (2002).
 8. M. Young, "Optical fiber index profiles by the refracted-ray method (refracted near-field scanning)," *Appl. Opt.* **20**(19), 3415–3422 (1981).
 9. Y. F. Chao and K. Y. Lee, "Index profile of radial gradient index lens measured by imaging ellipsometric technique," *Jpn. J. Appl. Phys.* **44**(2), 1111–1114 (2005).
 10. T. Q. Sun, Q. Ye, X. W. Wang, J. Wang, Z. C. Deng, J. C. Mei, W. Y. Zhou, C. P. Zhang, and J. G. Tian, "Scanning focused refractive-index microscopy," *Sci. Rep.* **4**, 5647 (2014).
 11. Y. Youk and D. Y. Kim, "Tightly focused epimicroscope technique for submicrometer-resolved highly sensitive refractive index measurement of an optical waveguide," *Appl. Opt.* **46**(15), 2949–2953 (2007).
 12. C. J. Weng, K. Y. Hsu, and Y. F. Chen, "Exploiting the image of the surface reflectivity to measure refractive index profiling for various optical fibers," *Opt. Express* **23**(9), 11755–11762 (2015).
 13. A. D. Yablou, "Multi-wavelength optical fiber refractive index profiling by spatially resolved Fourier transform spectroscopy," *J. Lightwave Technol.* **28**(4), 360–364 (2010).
 14. J. W. Fleming, "Dispersion in GeO₂-SiO₂ glasses," *Appl. Opt.* **23**(24), 4486–4493 (1984).
-

1. Introduction

Gradient-index (GRIN) rods are widely used to collimate or refocus incident light in applications including sensor, microendoscopy [1,2], and fiber telecommunication [3]. The wavelength range of these applications generally covers from visible to near IR region. Since the characteristics of a GRIN rod are mainly determined by the refractive-index distribution and material dispersion, it is highly demanded to develop a method for measuring the multi-wavelength refractive index profiles (RIPs) and dispersion. In the past, the proposed approaches for measuring the RIPs of GRIN rods consist of interferometry [4,5], focusing method [6,7], refracted near-field method [8], ellipsometric technique [9], and reflective scanning method [10–12]. Nevertheless, these methods for determining the multiple-wavelength RIPs usually require repeated measurements for different wavelengths. Recently, a different transverse interferometric method with a Fourier transform spectroscopy was proposed to measure the multi-wavelength RIPs of a 125- μm optical fiber that was inserted into the refractive index matching oil [13]. This transverse interferometric method may be extended to measure the multi-wavelength RIPs of the GRIN rod (mm in diameter). However, this method often takes a relative long time for phase unwrapping and computer processing. On the other hand, the variation of the refractive index of the GRIN rod depends on the dopant concentration of germanium (Ge). Therefore, it is highly desirable to develop a straightforward method for measuring the multi-wavelength RIPs of the GRIN rods and the dependence on the Ge-doped concentrations.

In this work, we develop a confocal microspectrophotometer (MSP) with a halogen lamp to directly scan the surface reflectivities on the end of the GRIN rod. The pure fused silica is used as a reference standard to deduce the absolute reflectivity of the Ge-doped core. The measured surface reflectivities are employed to obtain the multi-wavelength RIPs and material dispersion in the range of 400 to 900 nm. The advantage of this method is that the RIPs and dispersion can be obtained with a single measurement. Besides, an energy dispersive spectrometer (EDS) is used to measure the distribution of Ge-doped concentrations. By using the measured RIPs and the Ge-doped distribution, the dependence of broadband refractive indices on the Ge-doped concentrations is explicitly constructed. We believe that the present method could be applied to not only GRIN rods but also fiber preforms for obtaining the multi-wavelength RIPs and material dispersion.

2. Principle and method

The test sample was a Ge-doped GRIN rod with a core size $\sim 1200\ \mu\text{m}$. Figure 1(a) shows the experimental setup for scanning reflected intensities from the front end of the GRIN rod. The configuration was based on a MSP whose measuring wavelengths covered from 400 to 900 nm. A white light from an 100-W halogen lamp passed through a confocal pinhole, a collimating lens, an apochromatically corrected (VIS-NIR) objective lens (Zeiss, EC Epiplan-Apochromat $10\times$, N.A. = 0.25) and then focused on the front end of the GRIN rod. The reflected beam was collected by the objective lens and then coupled into a TE-cooled spectrometer (B&W Tek, BRC642E, 2 nm resolution) via a delivering multi-mode fiber patch (Thorlabs, M41L, 600 μm). The spectrometer had a high dynamic range of 33,000:1 and a 16 bits A/D converter. The core of the fiber patch played a role of another pinhole to satisfy the confocal condition with the confocal pinhole on the front end of GRIN rod. A color CCD (QImaging, MicroPublisher 5.0 RTV) was employed to capture the image of the GRIN rod. The front end of the GRIN rod was precisely cut with a 0° face angle and then polished into the condition of surface flatness $< \lambda/2$ at the wavelength of 632 nm. The picture of the polished front end of the GRIN rod was shown in Fig. 1(b). The GRIN rod consists of a core and two cladding layers. The core was the fused silica doped with Ge for raising the refractive index. The inner cladding was the F-doped material for decreasing the refractive index and the outer cladding was the pure fused silica material. From the specification of the vendor, the Ge-doped concentrations was approximately 13 mol. % at the core center and the F-doped concentrations was approximately 0.5 mol. % in the inner cladding. Furthermore, to

effectively reduce the return light, the backside end of the GRIN rod was well polished with a 60° face angle. Thus, the reflective light was reflected to the outside as shown in Fig. 1(a). The backside end of the GRIN rod with side polishing served as a terminator. Consequently, reflected intensity from the front end of the GRIN rod measured by the MSP was proportional to the spatially dependent refractive index.

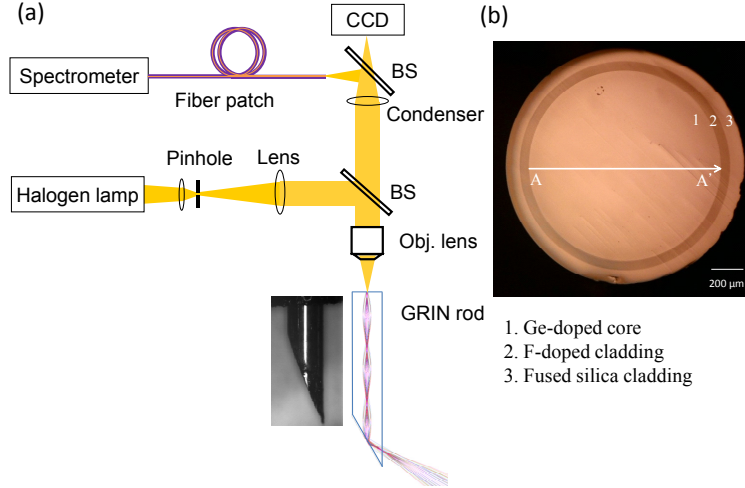


Fig. 1. (a) Scheme of the experimental setup for scanning surface reflectivities on the GRIN rod comprising a halogen lamp, pinhole, objective lens, CCD and spectrometer. (b) The end-surface picture of the polished GRIN rod.

The pure fused silica was usually used as a reference standard to determine the RIP of optical fiber. The refractive index of fused silica $n_{SiO_2}(\lambda)$ is well known in the range from VIS to NIR and can be expressed as the form of Sellmeier equation [14]:

$$n_{SiO_2}(\lambda) = \sqrt{1 + \sum_{i=1}^3 \frac{A_i \lambda^2}{\lambda^2 - l_i^2}} \quad \text{with} \quad A_i = \begin{pmatrix} 0.6961663 \\ 0.4079426 \\ 0.8974794 \end{pmatrix} \quad \text{and} \quad l_i = \begin{pmatrix} 0.0684043 \\ 0.1162414 \\ 9.8961610 \end{pmatrix}. \quad (1)$$

Substituting Eq. (1) into the Fresnel equation, the reflectivity of the fused silica, $R_{SiO_2}(\lambda)$, can be calculated. By using the calculated $R_{SiO_2}(\lambda)$ as a reference, the absolute surface reflectivities for the test GRIN rod, $R_{GRIN_rod}(r, \lambda)$, can be written as

$$R_{GRIN_rod}(r, \lambda) = R_{SiO_2}(\lambda) \frac{I_{GRIN_rod}(r, \lambda) - I_{background}(\lambda)}{I_{SiO_2}(\lambda) - I_{background}(\lambda)}, \quad (2)$$

where λ is the test wavelength, r is the radial position on the end of GRIN rod, $I_{background}(\lambda)$ is the dark background of the MSP, $I_{SiO_2}(\lambda)$ and $I_{GRIN_rod}(r, \lambda)$ are the spectral intensities of the illumination light through the objective lens and reflected from the fused silica cladding and the core of the GRIN rod, respectively. Therefore, the determined surface reflectivities $R_{GRIN_rod}(r, \lambda)$ on a core of the test GRIN rod can be used to further deduce the refractive index distribution. Substituting the determined $R_{GRIN_rod}(r, \lambda)$ into the inverse form of the Fresnel equation, the broadband refractive indices on a GRIN rod $n_{GRIN_rod}(r, \lambda)$ can be obtained by

$$n_{GRIN_rod}(r, \lambda) = \frac{1 + \sqrt{R_{GRIN_rod}(r, \lambda)}}{1 - \sqrt{R_{GRIN_rod}(r, \lambda)}}. \quad (3)$$

On the other hand, the uncertainty of the present method for determining refractive index, $\delta n_{GRIN_rod}(r, \lambda)$, is mainly caused by the error of the measured surface reflectivities $\delta R_{GRIN_rod}(r, \lambda)$. From Eq. (3), the relation between $\delta n_{GRIN_rod}(r, \lambda)$ and $\delta R_{GRIN_rod}(r, \lambda)$ can be written as

$$\delta n_{GRIN_rod}(r, \lambda) = \frac{(1 + n_{GRIN_rod}(r, \lambda))^3}{4(n_{GRIN_rod}(r, \lambda) - 1)} \delta R_{GRIN_rod}(r, \lambda) \quad (4)$$

In experiment, $\delta R_{GRIN_rod}(r, \lambda)$ is primarily caused from the power instability of the halogen lamp. The power instability is measured to be smaller than 0.5% in the range of 400-900 nm during testing time of 5 minutes. As a result, the measuring accuracy of refractive index can be better than 1.6×10^{-3} based on the proposed spectroscopy method of the surface reflectivity. Although the accuracy of this method is slightly inferior to the previous approaches, the multi-wavelength RIPs can be obtained simultaneously.

3. Experimental results and discussions

First, the broadband MSP was used to measure the surface reflectivities of the GRIN rod. The focused beam size of halogen lamp on the end of the GRIN rod was approximately 60 μm . In principle, the beam size does not have any effect on the accuracy of measured refractive index. Figure 2(a) shows the experimental results for the reflective intensities of the GRIN rod with a setting of 300 ms integrating time and 10 average numbers. All curves in the Fig. 2(a) had been subtracted with the dark background $I_{background}(\lambda)$. The maximum spectral response located at the wavelength of nearly 680 nm. There were a few small oscillations in three curves from 800 to 900 nm because of the absorption of OH⁻ inside the core of the delivering fiber patch. It will result in larger fluctuations of the broadband refractive indices. The higher intensity for the Ge-doped core center $I_{Ge-doped\ core\ center}$, the pink curve in Fig. 2(a), was caused by the higher refractive index. According to the lower refractive index caused by F doping, the reflective intensity of the F-doped cladding $I_{F-doped\ cladding}$ (green curve) was slight smaller than that of the fused silica cladding I_{SiO_2} (black curve). With Eqs. (2) and (3), the broadband refractive indices for core center of the Ge-doped and F-doped cladding can be obtained. Figure 2(b) shows the deduced broadband refractive indices and their fitting curves. It can be seen that the broadband refractive indices of Ge-doped core center is consistent with the Sellmeier fitting curve used in [14] except for a fluctuation in the range of 800 nm to 900 nm. From the experimental results, refractive-index difference between the core center and F-doped cladding Δn was approximately 0.022 at the wavelength of 630 nm. The refractive index of F-doped cladding was ~ 0.002 smaller than the reference value of the fused silica cladding at the same wavelength. As a result, the numerical aperture (N.A.) can be calculated to be approximately 0.255 at 630 nm which agrees very well with the N.A. of 0.25 ± 0.01 from the specification of the vendor.

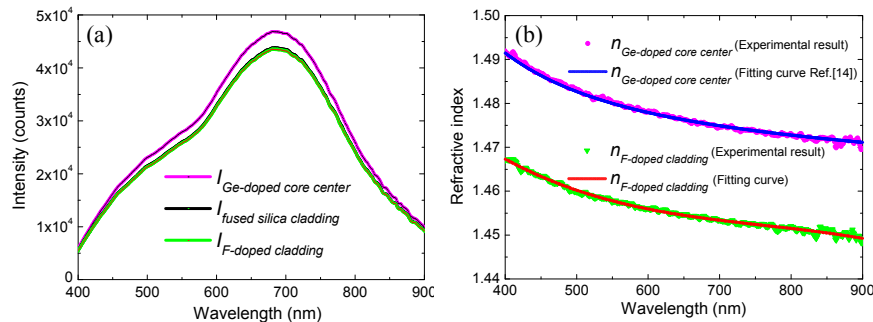


Fig. 2. (a) Reflective intensities for the Ge-doped core center, F-doped cladding and fused silica cladding. (b) Broadband refractive indices in the core center and the F-doped cladding and their fitting curves.

Next, this MSP scanned the radial position of the GRIN rod between two points A and A' in Fig. 1(b) with a spacing of 60 μm to record the multi-wavelength RIPs of the GRIN rod. The integration time was 300 ms and total scanning time was within 5 minutes. With the proposed analysis procedures, the one-dimensional RIPs of the GRIN rod at the nine wavelengths were obtained as shown in Fig. 3(a). The curves for the shorter wavelengths have the higher values of refractive index because of the natural material dispersion. The refractive index of the core center is in the range of 1.468 - 1.492 while the refractive index of the core edge is in the range of 1.449 - 1.471. It is more dispersive in the core center than that in the core edge because the variation of the refractive index depends on the Ge dopant concentration. Besides, the spatially dependent concentration was measured by using an EDS. A manual line-scan process was used to measure points every 67 μm across Ge-doped core. Referring to Fig. 3(b), it is clear that the ratio of Ge-doped concentration in the core was the graded distribution. It can be seen that the ratio of Ge-doped concentrations of the GRIN rod shows a good agreement with a parabola fitting curve. Since the core center is 13 mol. % GeO_2 concentrations, the spatial dependent concentrations on the cross-section of GRIN rod can be deduced from the fitting curve. Therefore, the relation between the broadband refractive indices and the Ge-doped concentrations can be connected easily. Figure 4(a) shows the broadband refractive indices of the GRIN rod with 4 different GeO_2 concentrations (1.7, 6.2, 9.5, and 13.0 mol. %). It can be seen that all curves have the similar shape with a shift in refractive index. After fitting experimental results, the material dispersion for the first derivative of the refractive index with respect to wavelength $dn/d\lambda$ for 4 GeO_2 concentrations can be calculated as shown in the Fig. 4(b). It can be found that all curves belong to negative dispersion and they are much dispersive in the visible range and the dispersion of Ge-doped silica core is highly dependent on the Ge-doped concentrations.

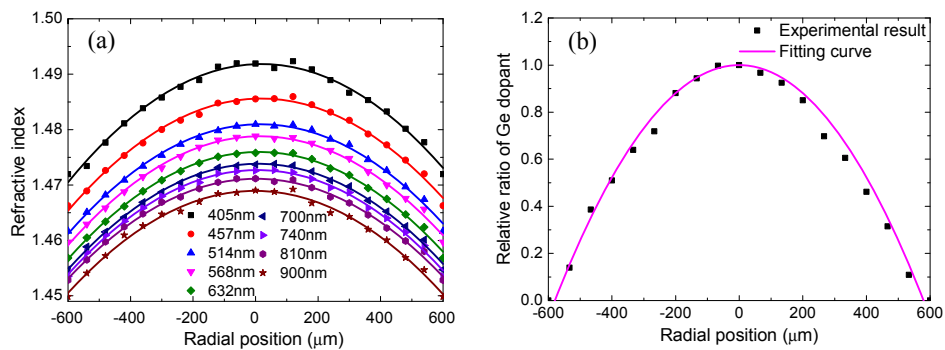


Fig. 3. (a) One-dimensional RIPs of the GRIN rod at the selected multiple wavelengths. (b) The spatially dependent profile of Ge-doped concentration on the GRIN core.

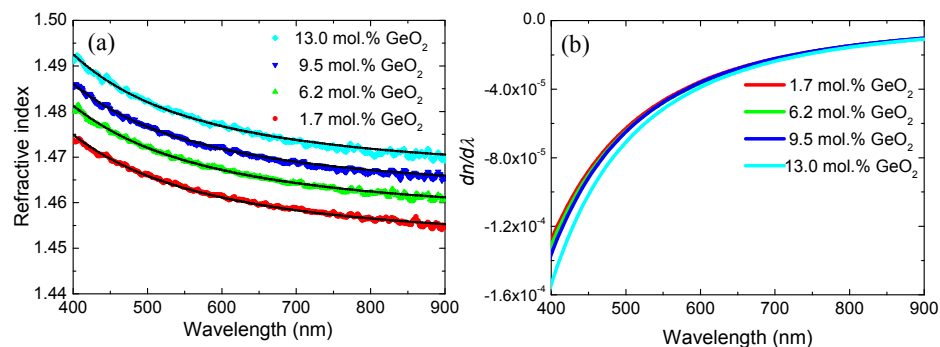


Fig. 4. (a) Broadband refractive indices in the core for different GeO_2 concentrations. (b) Dependence of $dn/d\lambda$ on wavelength for different GeO_2 concentrations.

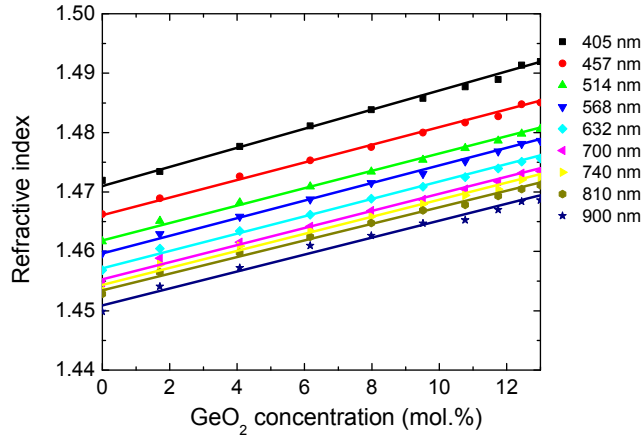


Fig. 5. Dependence of refractive index on the GeO₂ concentrations at nine wavelengths.

Finally, we make a quantitative connection between the refractive indices of GRIN rod at different wavelengths and the concentrations of GeO₂. Figure 5 shows the dependence of refractive index on doping concentration at the nine selected wavelengths. It can be found that the refractive indices are almost linear proportional to the doping concentrations and the slope of the curve at the short wavelength is slightly larger than that at the long wavelength. The slope $dn(\lambda)/dC$ is in the range of $1.42 \times 10^{-3} - 1.61 \times 10^{-3}$ /mol. % in the range of 400 to 900 nm. Furthermore, we develop an empiric formula to describe the dependence of refractive index on the concentrations of GeO₂ based on the refractive index of fused silica $n_{SiO_2}(\lambda)$ as a reference. The refractive index of Ge-doped GRIN rod $n_{GeO_2}(\lambda, C)$ can be written as

$$n_{GeO_2}(\lambda, C) = n_{SiO_2}(\lambda) + C \cdot dn(\lambda)/dC \quad \text{with} \quad dn(\lambda)/dC = \sum_{s=0}^3 a_s \cdot \lambda^s, \quad (5)$$

where C is the concentrations of GeO₂ (in mol. %) and the a_s is the coefficients of the polynomial equation. From fitting of the experimental results, the coefficients can be obtained with $a_0 = 1.9 \times 10^{-3}$, $a_1 = -1.2 \times 10^{-3}$, $a_2 = 1.0 \times 10^{-3}$, and $a_3 = -2.8 \times 10^{-4}$. With Eq. (5), the broadband refractive indices of the GRIN rod with the certain Ge-doped concentrations can be easily obtained.

4. Conclusion

In summary, we have successfully developed a confocal MSP with a halogen lamp to determine the multi-wavelength RIPs and material dispersion of a GRIN rod by scanning the surface reflectivities of the GRIN rod with pure fused silica as a reference standard. With the apochromatically corrected optics design, the measuring wavelength is broadband in the range from 400 to 900 nm and the accuracy of refractive index is better than 1.6×10^{-3} . Besides, an EDS is used to scan the distribution of Ge-doped concentrations. With the measured distribution, the dependence of broadband refractive indices on the Ge-doped concentrations is precisely constructed. As a result, the relation between the refractive index and the Ge-doped concentrations of the GRIN rod at a certain wavelength can be easily expressed as a linear form. By using the proposed method and the MSP, the spatially dependent Ge-doped concentrations, the material dispersion and multi-wavelength RIPs of a Ge-doped GRIN rod can be directly determined.

Acknowledgments

This work was sponsored in part by the Ministry of Science and Technology, Taiwan, R.O.C. under contract numbers MOST 103-2122-M-009-016-MY3 and 103-2622-E-492-019-CC3.